Exact solutions for social and biological contagion models on mixed directed and undirected, degree-correlated random networks

Joshua L. Payne,[1,*] Kameron Decker Harris,[2,3,†] and Peter Sheridan Dodds[2,3,‡]

[1]*Computational Genetics Laboratory, Dartmouth College, Hanover, New Hampshire 03755, USA*

[2]*Department of Mathematics & Statistics, The University of Vermont, Burlington, Vermont 05401, USA*

[3]*Complex Systems Center & the Vermont Advanced Computing Center, The University of Vermont, Burlington, Vermont 05401, USA*

(Received 28 February 2011; published 25 July 2011)

We derive analytic expressions for the possibility, probability, and expected size of global spreading events starting from a single infected seed for a broad collection of contagion processes acting on random networks with both directed and undirected edges and arbitrary degree-degree correlations. Our work extends previous theoretical developments for the undirected case, and we provide numerical support for our findings by investigating an example class of networks for which we are able to obtain closed-form expressions.

DOI: 10.1103/PhysRevE.84.016110 PACS number(s): 89.75.Hc, 64.60.aq, 87.23.Ge, 05.45.−a

I. INTRODUCTION

Spreading mechanisms playing out on generalized random networks constitute a rich and compelling class of tractable contagion models [1,2]. First, while real world complex networks are rarely, if ever, pure Erdős-Rényi networks, they often possess a strong, describable measure of randomness [3], once the dominant aspect of degree distribution is acknowledged [4]. Second, simple models of network-based spreading have yielded important insights into spreading phenomena such as the spread of infectious diseases [5,6], cascading failures in power grids [7,8], and social contagion processes [9–18]. Finally, many random network models are amenable to analytic investigations and researchers have naturally built on areas of statistical mechanics—with its great tradition of exactly solvable models—such as the study of percolation on lattices [19].

Here we examine contagion processes acting on mixed directed and undirected degree-assortative random networks. Specifically, for the case of a single seed, we derive and verify by simulations analytic expressions for three key aspects of these systems: (1) the *possibility* of a global spreading event; (2) the *probability* of a global spreading event; and (3) the *expected final size* of a successful global spreading event. We make the distinction between possibility and probability, the former referring to the potential for spreading (i.e., whether or not the system is in a phase where spreading may occur), and the latter to the quantified chance that a macroscopic spreading event may arise given the nature of the initial seed (e.g., random or targeted). Possibility is a categorical yes/no criterion and probability is a quantitative one; they ask different kinds of questions, and elicit different kinds of analyses for their determination. Thus, while we could simply derive the probability of global spreading only and thereby immediately know if global spreading was possible or not (corresponding to nonzero or zero probabilities), obtaining the possibility of global spreading alone is important as it directly reveals phase transitions, and further involves a transparent, physically argued calculation [20].

We base our work most strongly on two groups of authors' findings: Boguñá and Serrano [21], who provided a general formulation for the networks we consider here; and Gleeson and Cahalane [22,23], who derived the final size of global spreading events for general contagion models on a wide array of network structures, including the social-like threshold model on random networks [12,15,24]. Our work is also related to that of Meyers *et al.* [25] who examined disease-spreading models on mixed directed and undirected uncorrelated networks; our analytic methods are essentially disjoint and we treat more general spreading mechanisms (e.g., social-like ones), while Meyers *et al.* explored various real-world applications.

We structure our paper as follows. In Sec. II, we define the family of random networks and contagion processes we investigate here; in Sec. III, we provide physically motivated expressions for the possibility and probability of global spreading events starting from a single seed; and in Sec. IV, we derive coupled evolution equations that describe the growth of a global spreading event, as well as yield the expected final size. In the appropriate limits, our equations collapse to those for various network subclasses involving purely directed or undirected links, and correlated or uncorrelated nodes. In Sec. V, we obtain exact results regarding spreading on a specific family of random networks, and validate them with output from simulations. We close with a few remarks in Sec. VI.

II. MODEL DESCRIPTION

A. Generalized random networks

We consider random networks containing undirected and directed links along with arbitrary correlations between nodes based on degrees. Following Boguñá and Serrano [21], we allow each node to have k_u undirected edges, k_i incoming directed edges, and k_o outgoing directed edges. We assume all edges are unweighted. We represent a node by the generalized degree vector $\vec{k} = [k_u, k_i, k_o]^T$, which we will refer to simply as a node's degree, and we write $P(\vec{k})$ for the degree distribution.

*joshua.payne@dartmouth.edu
†kameron.harris@uvm.edu
‡peter.dodds@uvm.edu

To account for correlations, three conditional probabilities are needed: $P^{(\mathrm{u})}(\vec{k}\,|\,\vec{k}')$, $P^{(\mathrm{i})}(\vec{k}\,|\,\vec{k}')$, and $P^{(\mathrm{o})}(\vec{k}\,|\,\vec{k}')$; these quantities give the chances that an edge starting at a degree $\vec{k}'$ node ends at a degree $\vec{k}$ node and is, respectively, undirected, incoming, or outgoing relative to the destination degree $\vec{k}$ node (note that this convention for directed edges is opposite that used in [21]).

For networks to be well defined (i.e., realizable), these probabilities must be constrained by two detailed balance equations. In determining the probability that an edge of a certain type runs between nodes of degree $\vec{k}$ and $\vec{k}'$, we must obtain the same result whether we start at the former or latter node. We write the probability that a randomly chosen edge is undirected and connects a degree $\vec{k}$ and degree $\vec{k}'$ node as $P^{(\mathrm{u})}(\vec{k},\vec{k}')$. Noting that the probability that a random end of a randomly selected undirected edge emanates from a degree $\vec{k}$ node is given by $\frac{k_{\mathrm{u}}P(\vec{k})}{\langle k_{\mathrm{u}}\rangle}$, we have that

$$\begin{aligned} P^{(\mathrm{u})}(\vec{k},\vec{k}') &= P^{(\mathrm{u})}(\vec{k}\,|\,\vec{k}')\frac{k'_{\mathrm{u}}P(\vec{k}')}{\langle k'_{\mathrm{u}}\rangle} \\ &= P^{(\mathrm{u})}(\vec{k}'\,|\,\vec{k})\frac{k_{\mathrm{u}}P(\vec{k})}{\langle k_{\mathrm{u}}\rangle} = P^{(\mathrm{u})}(\vec{k}',\vec{k}). \end{aligned} \tag{1}$$

For directed edges we define $P^{(\mathrm{dir})}(\vec{k},\vec{k}')$ as the probability that a randomly chosen edge is directed and leads from a degree $\vec{k}'$ node to a degree $\vec{k}$ node. Similar to the balance equation for undirected edges, we use the quantities $\frac{k_{\mathrm{o}}P(\vec{k})}{\langle k_{\mathrm{o}}\rangle}$ and $\frac{k_{\mathrm{i}}P(\vec{k})}{\langle k_{\mathrm{i}}\rangle}$ which give the probabilities that in starting at a random end of a randomly selected edge, we begin at a degree $\vec{k}$ node and then find ourselves traveling (1) along an outgoing edge or (2) against the direction of an incoming edge. We therefore have

$$P^{(\mathrm{dir})}(\vec{k},\vec{k}') = P^{(\mathrm{i})}(\vec{k}\,|\,\vec{k}')\frac{k'_{\mathrm{o}}P(\vec{k}')}{\langle k'_{\mathrm{o}}\rangle} = P^{(\mathrm{o})}(\vec{k}'\,|\,\vec{k})\frac{k_{\mathrm{i}}P(\vec{k})}{\langle k_{\mathrm{i}}\rangle}. \tag{2}$$

Note that since $\langle k_{\mathrm{u}}\rangle = \langle k'_{\mathrm{u}}\rangle$ and $\langle k'_{\mathrm{o}}\rangle = \langle k_{\mathrm{o}}\rangle = \langle k_{\mathrm{i}}\rangle$, the denominators in Eqs. (1) and (2) are equal and may be omitted [21]. Furthermore, our alternate definitions of $P^{(\mathrm{i})}(\vec{k}'\,|\,\vec{k})$ and $P^{(\mathrm{o})}(\vec{k}'\,|\,\vec{k})$ mean that Eq. (2) has a form different to that given in [21].

For the class of random networks given above, Boguñá and Serrano determine a number of structural results regarding percolation, including the sizes of the giant in-component, out-component, and strongly connected component [21]. Our goal here is to examine the behavior of generalized spreading processes on such networks, and we describe these next.

B. Contagion processes

We consider synchronous discrete time contagion processes, though our results can at least in part be extended to asynchronous discrete and continuous time processes [20,23]. We assume that once nodes are infected, they remain so permanently, an aspect that is needed for computing the final size of a global spreading event. We write the probability of node j becoming infected in time step $t+1$ as

$$\mathcal{B}_j(k_{\mathrm{inf}};k_{\mathrm{u}}+k_{\mathrm{i}}), \tag{3}$$

given that k_{inf} of node j's total of $k_{\mathrm{u}}+k_{\mathrm{i}}$ undirected and incoming edges emanate from infected nodes at time t. Here, $\mathcal{B}_j$ is an arbitrary, node-specific "response function" mapping to the unit interval. Now, for the general class of contagion models we consider here on infinite random networks, we need to know only the average response function for each node subclass. Taking all nodes of degree $\vec{k}$, having indices in the set $J_{\vec{k}} = \{j_{\vec{k},1}, j_{\vec{k},2}, \ldots, j_{\vec{k},n}, \ldots\}$, we compute this average response function as

$$B_{k_{\mathrm{inf}},\vec{k}} = \lim_{n\to\infty}\frac{1}{n}\sum_{j=j_{\vec{k},1}}^{j_{\vec{k},n}}\mathcal{B}_j(k_{\mathrm{inf}};k_{\mathrm{u}}+k_{\mathrm{i}}). \tag{4}$$

The quantity $B_{k_{\mathrm{inf}},\vec{k}}$ is then the probability that a randomly chosen node of degree $\vec{k}$ is infected at time $t+1$ given that at time t, it has k_{inf} infected incoming and undirected edges.

III. POSSIBILITY AND PROBABILITY OF GLOBAL SPREADING

In [20], we derived a global spreading condition for discrete and continuous time contagion processes with the possibility of recovery acting on generalized random networks. Defining $\vec{\alpha} = (\nu,\lambda)$ to represent a pairing of a type ν node and type λ edge, we argued that the number of infected node-edge pairs $f_{\vec{\alpha}}$ grows as a function of network distance d from a seed as $f_{\vec{\alpha}}(d+1) = \sum_{\vec{\alpha}'} R_{\vec{\alpha}\vec{\alpha}'} f_{\vec{\alpha}'}(d)$, where $R_{\vec{\alpha}\vec{\alpha}'}$ depends simply on network structure and the spreading process [20]. As a special but still broad case, we showed that for the networks we consider here, the growth rate equation for the number of infected edges emanating from degree $\vec{k}$ nodes a distance d from an initiating node obeys the following:

$$\begin{bmatrix} f^{(\mathrm{u})}_{\vec{k}}(d+1) \\ f^{(\mathrm{o})}_{\vec{k}}(d+1) \end{bmatrix} = \sum_{k'}\mathbf{R}_{\vec{k}\vec{k}'}\begin{bmatrix} f^{(\mathrm{u})}_{\vec{k}'}(d) \\ f^{(\mathrm{o})}_{\vec{k}'}(d) \end{bmatrix}, \tag{5}$$

where

$$\mathbf{R}_{\vec{k}\vec{k}'} = \begin{bmatrix} P^{(\mathrm{u})}(\vec{k}\,|\,\vec{k}')\bullet(k_{\mathrm{u}}-1) & P^{(\mathrm{i})}(\vec{k}\,|\,\vec{k}')\bullet k_{\mathrm{u}} \\ P^{(\mathrm{u})}(\vec{k}\,|\,\vec{k}')\bullet k_{\mathrm{o}} & P^{(\mathrm{i})}(\vec{k}\,|\,\vec{k}')\bullet k_{\mathrm{o}} \end{bmatrix}\bullet B_{1,\vec{k}}. \tag{6}$$

Here the quantities $f^{(\mathrm{u})}_{\vec{k}}(d)$ and $f^{(\mathrm{o})}_{\vec{k}}(d)$ are the number of "infected" undirected and outgoing edges leaving an infected degree $\vec{k}$ node a distance d steps from the seed. We have expressed the form of $\mathbf{R}_{\vec{k}\vec{k}'}$ so as to make clear the three components making up general spreading conditions: (1) probability of connection [$P^{(\mathrm{u})}(\vec{k}\,|\,\vec{k}')$ and $P^{(\mathrm{i})}(\vec{k}\,|\,\vec{k}')$]; (2) resultant newly infected edges [$(k_{\mathrm{u}}-1)$, k_{u}, and k_{o} factors]; and (3) the probability of infection ($B_{1,\vec{k}}$) [20]. The above agrees with the contagion condition found earlier by Boguñá and Serrano for the emergence of the giant out-component using a generating function approach. Note that these calculations depend on the local pure branching structure of random networks with zero clustering; for recent advances for the nonzero clustering case see [26–29].

The full gain matrix $\mathbf{R}$ and edge infection counts $\vec{f}(d)$ can be laid out as follows:

$$\mathbf{R} = \begin{bmatrix} \mathbf{R}_{\vec{k}_1\vec{k}_1} & \mathbf{R}_{\vec{k}_1\vec{k}_2} & \cdots \\ \mathbf{R}_{\vec{k}_2\vec{k}_1} & \mathbf{R}_{\vec{k}_2\vec{k}_2} & \cdots \\ \vdots & \vdots & \ddots \end{bmatrix} \text{ and } \vec{f}(d) = \begin{bmatrix} f^{(\mathrm{u})}_{\vec{k}_1}(d) \\ f^{(\mathrm{o})}_{\vec{k}_1}(d) \\ f^{(\mathrm{u})}_{\vec{k}_2}(d) \\ f^{(\mathrm{o})}_{\vec{k}_2}(d) \\ \vdots \end{bmatrix}. \quad (7)$$

The condition for the possibility of global spreading events is therefore that the maximum eigenvalue of $[\mathbf{R}_{\vec{k}\vec{k}'}]$ exceeds 1:

$$\sup\{|\mu| : \mu \in \sigma([\mathbf{R}_{\vec{k}\vec{k}'}])\} > 1, \quad (8)$$

where $\sigma(\cdot)$ indicates spectrum.

Next, we determine the probability of a global spreading event given the initial seed is of degree $\vec{k}$ and hence the overall probability given a randomly selected seed; we refer to these quantities as "triggering" probabilities. While in determining the probability of a global spreading event we must also determine the possibility, the direct calculation we have just presented for the latter is needed to demonstrate a physically motivated clarity.

We define $Q^{(\mathrm{u})}_{\vec{k}}$ to be the probability that an infected undirected edge leaving a degree $\vec{k}$ node will lead to a giant component of infected nodes. Similarly, we define $Q^{(\mathrm{o})}_{\vec{k}}$ to be the probability that an infected outgoing edge from a degree $\vec{k}$ node will generate a global spreading event. Using the Markov nature of random networks, we can write down recursive, closed-form relationships for these two probabilities:

$$Q^{(\mathrm{u})}_{\vec{k}} = \sum_{\vec{k}'} P^{(\mathrm{u})}(\vec{k}'\,|\,\vec{k})\big[1 - \big(1 - Q^{(\mathrm{u})}_{\vec{k}'}\big)^{k'_{\mathrm{u}}-1}\big(1 - Q^{(\mathrm{o})}_{\vec{k}'}\big)^{k'_{\mathrm{o}}}\big]B_{1,\vec{k}'} \quad (9)$$

and

$$Q^{(\mathrm{o})}_{\vec{k}} = \sum_{\vec{k}'} P^{(\mathrm{i})}(\vec{k}'\,|\,\vec{k})\big[1 - \big(1 - Q^{(\mathrm{u})}_{\vec{k}'}\big)^{k'_{\mathrm{u}}}\big(1 - Q^{(\mathrm{o})}_{\vec{k}'}\big)^{k'_{\mathrm{o}}}\big]B_{1,\vec{k}'}. \quad (10)$$

In these equations we have encoded the understanding that if an infected edge generates a global spreading event, then it must infect its target node which in turn must be successful in infecting its other neighbors. In Eq. (10), for example, $P^{(\mathrm{i})}(\vec{k}'\,|\,\vec{k})$ is the probability that the undirected edge leads from an infected degree $\vec{k}$ node to a degree $\vec{k}'$ node which it infects with probability $B_{1,\vec{k}'}$. The quantity $(1 - Q^{(\mathrm{u})}_{\vec{k}'})^{k'_{\mathrm{u}}}(1 - Q^{(\mathrm{o})}_{\vec{k}'})^{k'_{\mathrm{o}}}$ is the probability that none of the infected node's other undirected or outgoing edges successfully spread the infection, and hence $[1 - (1 - Q^{(\mathrm{u})}_{\vec{k}'})^{k'_{\mathrm{u}}}(1 - Q^{(\mathrm{o})}_{\vec{k}'})^{k'_{\mathrm{o}}}]$ is the probability that at least one does.

Both $Q^{(\mathrm{u})}_{\vec{k}}$ and $Q^{(\mathrm{o})}_{\vec{k}}$ can be determined from Eqs. (9) and (10) either numerically or exactly (as per our example later in Sec V). Having done so, we can then compute the probability that infecting a single degree $\vec{k}$ node triggers a global spreading event:

$$P_{\mathrm{trig}}(\vec{k}) = \big[1 - \big(1 - Q^{(\mathrm{u})}_{\vec{k}}\big)^{k_{\mathrm{u}}}\big(1 - Q^{(\mathrm{o})}_{\vec{k}}\big)^{k_{\mathrm{o}}}\big], \quad (11)$$

which is the complement of $(1 - Q^{(\mathrm{u})}_{\vec{k}})^{k_{\mathrm{u}}}(1 - Q^{(\mathrm{o})}_{\vec{k}})^{k_{\mathrm{o}}}$, the probability of failure to trigger. The probability that infecting a randomly chosen node triggers a global spreading event is then simply $P_{\mathrm{trig}} = \sum_{\vec{k}} P_{\mathrm{trig}}(\vec{k})$, or

$$P_{\mathrm{trig}} = \sum_{\vec{k}} P(\vec{k})\big[1 - \big(1 - Q^{(\mathrm{u})}_{\vec{k}}\big)^{k_{\mathrm{u}}}\big(1 - Q^{(\mathrm{o})}_{\vec{k}}\big)^{k_{\mathrm{o}}}\big]. \quad (12)$$

In similar fashion, the triggering probability for nonrandom, strategic selections of the initial seed can readily be obtained. Appropriate limits of Eq. (12) also recover triggering probabilities for simpler families of random networks such as undirected, uncorrelated networks with prescribed degree distributions. Finally, considering the limit of $P_{\mathrm{trig}} \to 0$ retrieves the condition for global spreading found above.

IV. FINAL SIZE OF SUCCESSFUL GLOBAL SPREADING EVENTS

We complete our main analysis by determining the final size of a global spreading event building on the work of Gleeson and Cahalane [22] and later Gleeson [23]. We shift our focus from spreading away from a seed (expansion) to spreading reaching a node (contraction).

We consider an arbitrary fixed node in the network and compute the probability that incoming edges (directed or undirected) are infected and sufficient in number that the node itself becomes infected at a certain time. To do so, we need to first determine the probabilities that undirected and incoming edges arriving at a degree $\vec{k}$ node are infected at time t, $\theta^{(\mathrm{u})}_{\vec{k},t}$ and $\theta^{(\mathrm{i})}_{\vec{k},t}$. As with the possibility and probability of spreading, edge-edge transitions are the best framing for this calculation. Edges will be infected at time $t+1$ if the node from which they emanate becomes infected in that time step, and this in turn depends on the infection levels of the incoming edges. Assuming a fraction $\phi_0 > 0$ of initially infected seeds in the network, we obtain the following expression for the fraction of infected directed and incoming edges in the network at time $t+1$:

$$\begin{aligned}\theta^{(\mathrm{u})}_{\vec{k},t+1} = \phi_0 + (1-\phi_0)\sum_{\vec{k}'} P^{(\mathrm{u})}(\vec{k}\,|\,\vec{k}')\sum_{j_{\mathrm{u}}=0}^{k'_{\mathrm{u}}-1}\sum_{j_{\mathrm{i}}=0}^{k'_{\mathrm{i}}}\binom{k'_{\mathrm{u}}-1}{j_{\mathrm{u}}}\binom{k'_{\mathrm{i}}}{j_{\mathrm{i}}} \\ \times\big[\theta^{(\mathrm{u})}_{\vec{k}',t}\big]^{j_{\mathrm{u}}}\big[1-\theta^{(\mathrm{u})}_{\vec{k}',t}\big]^{(k'_{\mathrm{u}}-1-j_{\mathrm{u}})}\big[\theta^{(\mathrm{i})}_{\vec{k}',t}\big]^{j_{\mathrm{i}}} \\ \times\big[1-\theta^{(\mathrm{i})}_{\vec{k}',t}\big]^{(k'_{\mathrm{i}}-j_{\mathrm{i}})}B_{j_{\mathrm{u}}+j_{\mathrm{i}},k'_{\mathrm{u}}+k'_{\mathrm{i}}}, \quad (13)\end{aligned}$$

and

$$\begin{aligned}\theta^{(\mathrm{i})}_{\vec{k},t+1} = \phi_0 + (1-\phi_0)\sum_{\vec{k}'} P^{(\mathrm{i})}(\vec{k}\,|\,\vec{k}')\sum_{j_{\mathrm{u}}=0}^{k'_{\mathrm{u}}}\sum_{j_{\mathrm{i}}=0}^{k'_{\mathrm{i}}}\binom{k'_{\mathrm{u}}}{j_{\mathrm{u}}}\binom{k'_{\mathrm{i}}}{j_{\mathrm{i}}} \\ \times\big[\theta^{(\mathrm{u})}_{\vec{k}',t}\big]^{j_{\mathrm{u}}}\big[1-\theta^{(\mathrm{u})}_{\vec{k}',t}\big]^{(k'_{\mathrm{u}}-j_{\mathrm{u}})}\big[\theta^{(\mathrm{i})}_{\vec{k}',t}\big]^{j_{\mathrm{i}}}\big[1-\theta^{(\mathrm{i})}_{\vec{k}',t}\big]^{(k'_{\mathrm{i}}-j_{\mathrm{i}})} \\ \times B_{j_{\mathrm{u}}+j_{\mathrm{i}},k'_{\mathrm{u}}+k'_{\mathrm{i}}}. \quad (14)\end{aligned}$$

Since we are now considering contraction rather than expansion, more than one edge may contribute to the infection of a node, hence the sum over nearly the full range of infection probabilities, the $\{B_{j_{\mathrm{u}}+j_{\mathrm{i}},k'_{\mathrm{u}}+k'_{\mathrm{i}}}\}$.

The overall fraction of infected nodes at time t, equivalently the probability that a randomly chosen node becomes infected at time t, depends on $\theta^{(\mathrm{u})}_{\vec{k}',t}$ and $\theta^{(\mathrm{i})}_{\vec{k}',t}$ as

$$\phi_{t+1} = \phi_0 + (1-\phi_0)\sum_{\vec{k}} P(\vec{k}) \sum_{j_\mathrm{u}=0}^{k_\mathrm{u}} \sum_{j_\mathrm{i}=0}^{k_\mathrm{i}} \binom{k_\mathrm{u}}{j_\mathrm{u}} \binom{k_\mathrm{i}}{j_\mathrm{i}} \times \left[\theta^{(\mathrm{u})}_{\vec{k},t}\right]^{j_\mathrm{u}} \left[1-\theta^{(\mathrm{u})}_{\vec{k},t}\right]^{(k_\mathrm{u}-j_\mathrm{u})} \left[\theta^{(\mathrm{i})}_{\vec{k},t}\right]^{j_\mathrm{i}} \left[1-\theta^{(\mathrm{i})}_{\vec{k},t}\right]^{(k_\mathrm{i}-j_\mathrm{i})} \times B_{j_\mathrm{u}+j_\mathrm{i},k_\mathrm{u}+k_\mathrm{i}}. \quad (15)$$

To determine the final size, we set $\theta^{(\mathrm{u})}_{\vec{k}',t+1} = \theta^{(\mathrm{u})}_{\vec{k}',t} = \theta^{(\mathrm{u})}_{\vec{k}',\infty}$ and $\theta^{(\mathrm{i})}_{\vec{k}',t+1} = \theta^{(\mathrm{i})}_{\vec{k}',t} = \theta^{(\mathrm{i})}_{\vec{k}',\infty}$ in Eqs. (13) and (14) and solve for the steady-state solutions $\theta^{(\mathrm{u})}_{\vec{k}',\infty}$ and $\theta^{(\mathrm{i})}_{\vec{k}',\infty}$. Substituting these values into Eq. (15) gives us the expected final size ϕ_∞ which is, among other things, a function of ϕ_0, the fraction of nodes initially infected. For the single seed case we consider in this present work, the final step therefore is to take the limit $\phi_0 \to 0$. Note that as for the triggering probability, the condition for global spreading, Eq. (8), can be recovered by linearizing Eqs. (13), (14), and (15) (see Ref. [23]).

V. EXACT SOLUTION FOR AN EXAMPLE DEGREE-CORRELATED RANDOM NETWORK WITH MIXED DIRECTED AND UNDIRECTED EDGES

To test our analytic expressions for the possibility, probability, and expected final size of a global spreading event, we consider a family of general random networks for which our equations are exactly solvable. As shown schematically in the margins of Fig. 1, we allow four types of nodes with the following degree vectors, which, again, have the form $\vec{k} = [k_\mathrm{u}, k_\mathrm{i}, k_\mathrm{o}]^\mathrm{T}$:

$$\vec{k}_1 = \begin{bmatrix} 2 \\ 1 \\ 1 \end{bmatrix}, \quad \vec{k}_2 = \begin{bmatrix} 0 \\ 0 \\ 1 \end{bmatrix}, \quad \vec{k}_3 = \begin{bmatrix} 0 \\ 1 \\ 0 \end{bmatrix}, \quad \text{and} \quad \vec{k}_4 = \begin{bmatrix} 1 \\ 0 \\ 0 \end{bmatrix}, \quad (16)$$

and which occur with abundances

$$P(\vec{k}_1) = \tfrac{1}{5}, \quad P(\vec{k}_2) = \tfrac{1}{5}, \quad P(\vec{k}_3) = \tfrac{1}{5}, \quad \text{and} \quad P(\vec{k}_4) = \tfrac{2}{5}. \quad (17)$$

We define the degree-degree conditional probabilities as dependent on two tunable parameters, τ_und and τ_dir:

$$[P^{(\mathrm{u})}(\vec{k} \mid \vec{k}')] = \begin{bmatrix} \tau_\mathrm{und} & 0 & 0 & (1-\tau_\mathrm{und}) \\ 0 & 0 & 0 & 0 \\ 0 & 0 & 0 & 0 \\ (1-\tau_\mathrm{und}) & 0 & 0 & \tau_\mathrm{und} \end{bmatrix} \quad (18)$$

and

$$[P^{(\mathrm{i})}(\vec{k} \mid \vec{k}')] = [P^{(\mathrm{o})}(\vec{k} \mid \vec{k}')]^\mathrm{T} = \begin{bmatrix} \tau_\mathrm{dir} & (1-\tau_\mathrm{dir}) & 0 & 0 \\ 0 & 0 & 0 & 0 \\ (1-\tau_\mathrm{dir}) & \tau_\mathrm{dir} & 0 & 0 \\ 0 & 0 & 0 & 0 \end{bmatrix}. \quad (19)$$

where $0 \leqslant \tau_\mathrm{dir}, \tau_\mathrm{und} \leqslant 1$, and $\vec{k}$ and $\vec{k}'$ correspond to rows and columns.

We have chosen τ_dir and τ_und so that increasing them will tend to increase global connectivity, with τ_und controlling correlations between nodes through undirected edges, and τ_dir through directed ones. There are four clear limiting cases, as shown in the corners of Fig. 1. For example, when $\tau_\mathrm{dir} = \tau_\mathrm{und} = 1$ (upper right corner of Fig. 1), type 1 nodes are connected only to other type 1 nodes creating a giant component, while the other three types combine to form isolated pairs with either directed or undirected connections. At the other extreme when $\tau_\mathrm{dir} = \tau_\mathrm{und} = 0$ (lower left corner of Fig. 1), each of the four edges from type 1 nodes connect only to type 2, 3, and 4 nodes, meaning the network is composed of discrete, five-node components. The six other example networks in Fig. 1 give a sense of the other possible configurations contained within this simple network family we have constructed.

We obtain results for general response functions, while for comparison with simulations, we consider a test contagion process with the following single-parameter threshold transmission probabilities:

$$B_{0,\vec{k}_i} = 0 \quad B_{1,\vec{k}_1} = \beta \quad \text{and} \quad B_{j,\vec{k}_i} = 1 \quad \text{otherwise.} \quad (20)$$

where $i = 1, \ldots, 4$. The choice $B_{0,\vec{k}_i} = 0$ means no nodes spontaneously become infected (as might model the action of an exogenous source of infection). In the case that $\beta = 1$, then this set of responses means that if a node finds at least one neighbor at the end of an undirected or incoming edge that is infected, then the node itself becomes infected in the next time step. For $\beta < 1$, a random fraction β of degree $\vec{k}_1$ nodes become infected in the time step following the infection of a single neighbor, whereas $1-\beta$ remain uninfected. As discussed in Sec. II B, individual response functions need only give this average response function; for example, a fraction β of degree $\vec{k}_1$ nodes might have a deterministic threshold of 1 with the remaining fraction of $1-\beta$ having a deterministic threshold of 2.

Returning to Fig. 1, the gray-scale plot shows the fractional size of successful global spreading events as a function of τ_und and τ_dir for the specific spreading mechanism described above with $\beta(= B_{1,\vec{k}_1}) = 1$. We see a clear phase transition indicated by the dashed curve and our next task is to find its analytic form.

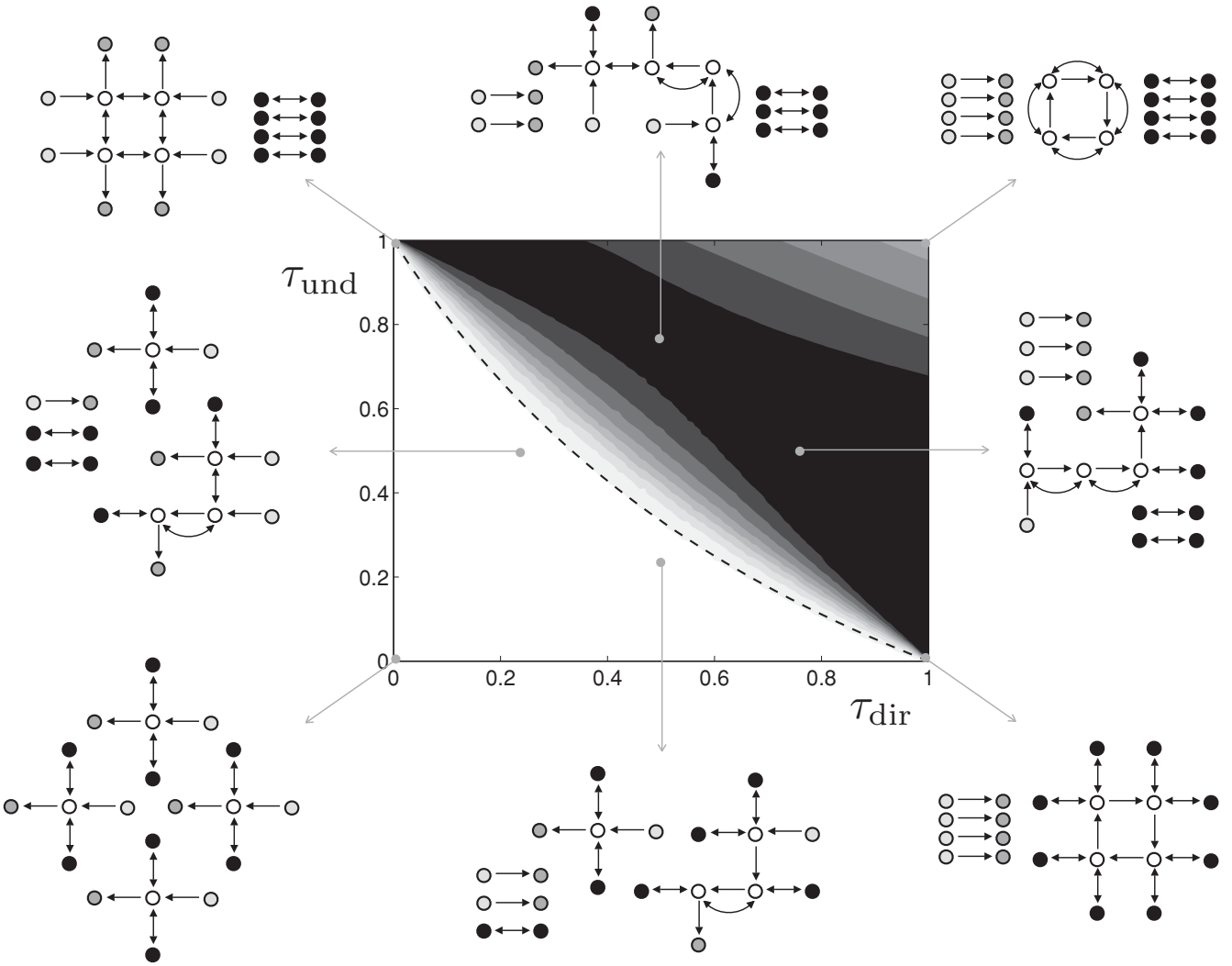

FIG. 1. Central plot: For the toy network model described in Sec. V, final size ϕ_∞ as a function of the model parameters $\tau_{\rm und}$ and $\tau_{\rm dir}$. Size is mapped to a linear gray scale with white indicating no global spreading. The dashed line marks the theoretically determined phase transition given in Eq. (22). The example networks shown around the plot give a sense of the kinds of networks realized for the corresponding $\tau_{\rm und}$ and $\tau_{\rm dir}$. Note that we show exact forms for networks with 20 nodes to make clear how node types are correlated in phase space, and forms will differ for larger networks. For example, for $\tau_{\rm und} = \tau_{\rm dir} = 1$, networks will comprise a giant component of type 1 nodes (open circles) with the remaining three node types represented only in isolated pairs. Simulation details: We formed each network with $N = 10^4$ nodes made up of a 1:1:1:2 ratio of node types 1 through 4. We constructed each network initially to have $\tau_{\rm und} = \tau_{\rm dir} = 1$, which was simple algorithmically, and then shuffled edges until desired values of $\tau_{\rm und}$ and $\tau_{\rm dir}$ were reached, using an approach similar to those described in [30] and [31]. We further shuffled each edge type 10 000 times to ensure randomization. For each $\tau_{\rm und}$ and $\tau_{\rm dir}$ in 0, 0.01, 0.02, . . . , 1.00, we generated 100 networks and randomly picked 1000 seeds for a total of 10^5 samples.

A. Global spreading condition

Using the spreading conditions contained in Eqs. (5), (7), and (8), and the model's definition, we find that global spreading may occur when the maximum eigenvalue of the following gain matrix exceeds unity:

$$\mathbf{R} = \begin{bmatrix} \mathbf{R}_{\vec{k}_1\vec{k}_1} & \mathbf{R}_{\vec{k}_1\vec{k}_2} & \mathbf{R}_{\vec{k}_1\vec{k}_3} & \mathbf{R}_{\vec{k}_1\vec{k}_4} \\ \mathbf{R}_{\vec{k}_2\vec{k}_1} & \mathbf{R}_{\vec{k}_2\vec{k}_2} & \mathbf{R}_{\vec{k}_2\vec{k}_3} & \mathbf{R}_{\vec{k}_2\vec{k}_4} \\ \mathbf{R}_{\vec{k}_3\vec{k}_1} & \mathbf{R}_{\vec{k}_3\vec{k}_2} & \mathbf{R}_{\vec{k}_3\vec{k}_3} & \mathbf{R}_{\vec{k}_3\vec{k}_4} \\ \mathbf{R}_{\vec{k}_4\vec{k}_1} & \mathbf{R}_{\vec{k}_4\vec{k}_2} & \mathbf{R}_{\vec{k}_4\vec{k}_3} & \mathbf{R}_{\vec{k}_4\vec{k}_4} \end{bmatrix} = \begin{bmatrix} \tau_{\rm und}B_{1,\vec{k}_1} & 2\tau_{\rm dir}B_{1,\vec{k}_1} & 0 & 2(1-\tau_{\rm dir})B_{1,\vec{k}_2} & 0 & 0 & (1-\tau_{\rm und})B_{1,\vec{k}_4} & 0 \\ \tau_{\rm und}B_{1,\vec{k}_1} & \tau_{\rm dir}B_{1,\vec{k}_1} & 0 & (1-\tau_{\rm dir})B_{1,\vec{k}_2} & 0 & 0 & (1-\tau_{\rm und})B_{1,\vec{k}_4} & 0 \\ 0 & 0 & 0 & 0 & 0 & 0 & 0 & 0 \\ \vdots & \vdots & \vdots & \vdots & \vdots & \vdots & \vdots & \vdots \\ 0 & 0 & 0 & 0 & 0 & 0 & 0 & 0 \end{bmatrix}. \quad (21)$$

Clearly, only the top left hand corner of this gain matrix matters as global spreading, if possible, must occur on a giant component. Upon substitution of the model's response functions given in Eq. (20), we find the largest eigenvalue is $\frac{1}{2}(\tau_{\text{und}} + \tau_{\text{dir}} + \sqrt{(\tau_{\text{und}} + \tau_{\text{dir}})^2 + 4\tau_{\text{und}}\tau_{\text{dir}}})\beta$ and we find that global spreading events therefore occur in the region described by

$$(1 + \tau_{\text{und}}\beta)(1 + \tau_{\text{dir}}\beta) > 2. \tag{22}$$

For the case $\beta(= B_{1,\vec{k}_1}) = 1$, this equation is indeed represented by the dashed curve shown in Fig. 1, perfectly matching the phase transition demonstrated by our simulations. We can also now readily determine that spreading may occur for some values of τ_{und} and τ_{dir} providing $\beta > \sqrt{2} - 1$.

B. Probability of global spreading

In computing the probability that a degree $\vec{k}$ node initiates a global spreading event, we observe that because only type 1 nodes can transmit an infection, we need only solve the recursion equations given in (9) and (10) for $Q^{(\text{u})}_{\vec{k}_1}$ and $Q^{(\text{o})}_{\vec{k}_1}$. Nodes of type 2 and 4, possessing one outgoing and one undirected edge, respectively, may trigger global spreading but obviously cannot be involved in transmission, and nodes of type 3 can neither start nor help spread an outbreak. Equations (9) and (10) reduce to the nonlinear coupled equations:

$$Q^{(\text{u})}_{\vec{k}_1} = \tau_{\text{und}}\left[1 - \left(1 - Q^{(\text{u})}_{\vec{k}_1}\right)\left(1 - Q^{(\text{o})}_{\vec{k}_1}\right)\right]\beta \tag{23}$$

and

$$Q^{(\text{o})}_{\vec{k}_1} = \tau_{\text{dir}}\left[1 - \left(1 - Q^{(\text{u})}_{\vec{k}_1}\right)^2\left(1 - Q^{(\text{o})}_{\vec{k}_1}\right)\right]\beta. \tag{24}$$

The equations are solvable and we find

$$Q^{(\text{u})}_{\vec{k}_1} = 1 + \frac{1}{2}\tau_{\text{und}}\beta - \sqrt{\frac{1}{4}(\tau_{\text{und}}\beta)^2 - \frac{\tau_{\text{und}}}{\tau_{\text{dir}}} + \frac{1}{\tau_{\text{dir}}\beta}}, \tag{25}$$

with

$$Q^{(\text{o})}_{\vec{k}_1} = \left(\frac{1}{\tau_{\text{und}}\beta} - 1\right)\frac{Q^{(\text{u})}_{\vec{k}_1}}{1 - Q^{(\text{u})}_{\vec{k}_1}}. \tag{26}$$

For $\beta = \tau_{\text{und}} = \tau_{\text{dir}} = 1$, $Q^{(\text{u})}_{\vec{k}_1} = Q^{(\text{o})}_{\vec{k}_1} = 1$. In turn, $Q^{(\text{o})}_{\vec{k}_2}$ and $Q^{(\text{u})}_{\vec{k}_4}$ can be expressed in terms of $Q^{(\text{u})}_{\vec{k}_1}$ and $Q^{(\text{o})}_{\vec{k}_1}$:

$$Q^{(\text{o})}_{\vec{k}_2} = (1 - \tau_{\text{dir}})\left[1 - \left(1 - Q^{(\text{u})}_{\vec{k}_1}\right)^2\left(1 - Q^{(\text{o})}_{\vec{k}_1}\right)\right]\beta \tag{27}$$

and

$$Q^{(\text{u})}_{\vec{k}_4} = (1 - \tau_{\text{und}})\left[1 - \left(1 - Q^{(\text{u})}_{\vec{k}_1}\right)\left(1 - Q^{(\text{o})}_{\vec{k}_1}\right)\right]\beta. \tag{28}$$

A first check on these triggering probability expressions is that they are in agreement with the phase transition recorded in Eq. (22); in other words, $Q^{(\text{u})}_{\vec{k}_1}$ and $Q^{(\text{o})}_{\vec{k}_1}$ should vanish along the phase transition. We see that upon setting the right-hand side of Eq. (25) to zero, rearrangement indeed leads to the condition $(1 + \tau_{\text{und}}\beta)(1 + \tau_{\text{dir}}\beta) = 2$.

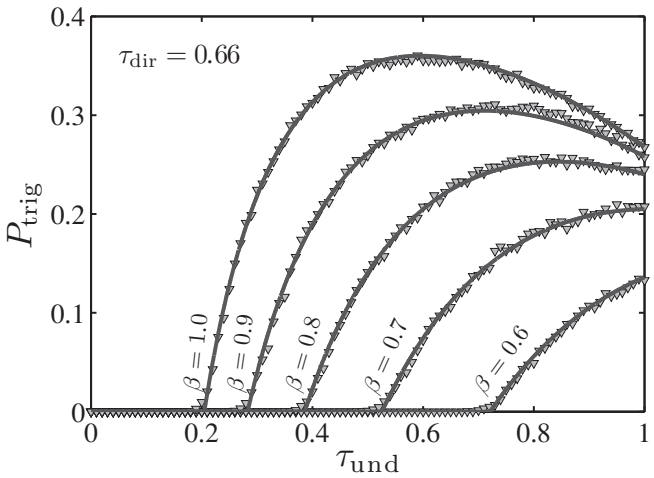

FIG. 2. For the model described in Sec. V, the probability that infecting a randomly chosen node leads to a global spreading event P_{trig} as a function of undirected edge assortativity τ_{und}, a fixed value of directed edge assortativity $\tau_{\text{dir}} = 0.66$, and varying values of $\beta = B_{1,\vec{k}_1}$. The curves correspond to output from simulations [squares] and theory [solid line, Eq. (29)]. For the simulation results we recorded a successful global spreading event if the final size exceeded 2.5% of the network. This cut off is arbitrary but nearby values do not appreciably change the resulting picture because above the phase transition the final size is bimodal: either spreading takes off and reaches a characteristic fraction of the network, or it fails. The network size is $N = 10^5$ and the resolution in τ_{und} is 0.01. See caption of Fig. 1 for further details.

We compute the triggering probability given a randomly chosen seed using Eq. (12):

$$P_{\text{trig}} = \tfrac{1}{5}\left[1 - \left(1 - Q^{(\text{u})}_{\vec{k}_1}\right)^2\left(1 - Q^{(\text{o})}_{\vec{k}_1}\right)\right] + \tfrac{1}{5}Q^{(\text{o})}_{\vec{k}_2} + \tfrac{2}{5}Q^{(\text{u})}_{\vec{k}_4}. \tag{29}$$

We compare our theoretical computation of P_{trig} with simulations in Fig. 2 for one transect in $\tau_{\text{und}} - \tau_{\text{dir}}$ parameter space ($\tau_{\text{dir}} = 0.66$, τ_{und} varying), and some example values of β.

Note that for $\beta = 1$ all nodes are vulnerable providing they can be reached along an edge, and the contagion model's behavior exhibits an inherent symmetry in the network's giant in-component and out-component, implying that $P_{\text{trig}} = \phi_\infty$. For the infection probability P_{trig}, the initial node must be part of the giant in-component which is made up of type 1, 2, and 4 nodes. The final infected component will match the giant out-component which is turn made up of type 1, 3, and 4 nodes. The giant strongly connected component is found in the intersection: type 1 and 4 nodes.

C. Final size of infection

We use the evolution equations given in Sec. IV to describe the growth of the spreading process on our example networks, with the main goal of determining the final size. We start with the equations for edge infection probabilities $\theta^{(\text{u})}_{\vec{k},t+1}$ and $\theta^{(\text{o})}_{\vec{k},t+1}$ [Eqs. (13) and (14)] and we present their full model-specific forms in the Appendix. We let $t \to \infty$ in these equations and solve for fixed points $\theta^{(\text{u})}_{\vec{k},\infty}$ and $\theta^{(\text{o})}_{\vec{k},\infty}$. Only two of the

eight possible equations are coupled, those for $\theta^{(\mathrm{i})}_{1,\infty}$ and $\theta^{(\mathrm{u})}_{1,\infty}$ [Eqs. (A1) and (A2)], and thus they alone determine the final probabilities. As per our previous calculations, this collapse in equation number is because $\vec{k}_1$ nodes are the only type capable of receiving and transmitting an infection. With these observations, and in setting $\beta = 1$ for simplicity, we obtain the coupled equations

$$\theta^{(\mathrm{u})}_{\vec{k}_1,\infty} = \tau_{\mathrm{und}}\left[\theta^{(\mathrm{u})}_{\vec{k}_1,\infty}\left(1-\theta^{(\mathrm{i})}_{\vec{k}_1,\infty}\right)+\theta^{(\mathrm{i})}_{\vec{k}_1,\infty}\right] \tag{30}$$

and

$$\theta^{(\mathrm{i})}_{\vec{k}_1,\infty} = \tau_{\mathrm{dir}}\left(\left[2\theta^{(\mathrm{u})}_{\vec{k}_1,\infty}-\left(\theta^{(\mathrm{u})}_{\vec{k}_1,\infty}\right)^2\right]\left[1-\theta^{(\mathrm{i})}_{\vec{k}_1,\infty}\right]+\theta^{(\mathrm{i})}_{\vec{k}_1,\infty}\right). \tag{31}$$

Solving both equations for $\theta^{(\mathrm{i})}_{\vec{k}_1,\infty}$ and equating the results leads to a cubic polynomial in $\theta^{(\mathrm{u})}_{\vec{k}_1,\infty}$. One root is $\theta^{(\mathrm{u})}_{\vec{k}_1,\infty} = 0$ and the others are solutions to

$$\begin{aligned} 0 = {} & \tau_{\mathrm{dir}}\left(\theta^{(\mathrm{u})}_{\vec{k}_1,\infty}\right)^2 - \tau_{\mathrm{dir}}(\tau_{\mathrm{und}}+2)\theta^{(\mathrm{u})}_{\vec{k}_1,\infty} \\ & +(\tau_{\mathrm{dir}}+1)(\tau_{\mathrm{und}}+1)-2. \end{aligned} \tag{32}$$

We look for solutions for which $0 \leqslant \theta^{(\mathrm{u})}_{\vec{k}_1,\infty} \leqslant 1$. If $(\tau_{\mathrm{dir}}+1)(\tau_{\mathrm{und}}+1) \leqslant 2$, we find the only feasible solution is $\theta^{(\mathrm{u})}_{\vec{k}_1,\infty} = 0$. When $(\tau_{\mathrm{dir}}+1)(\tau_{\mathrm{und}}+1) > 2$ we find $\theta^{(\mathrm{u})}_{\vec{k}_1,\infty} = 0$ again but now also a nontrivial solution:

$$\theta^{(\mathrm{u})}_{\vec{k}_1,\infty} = \frac{1}{2}(\tau_{\mathrm{und}}+2)\left[1-\sqrt{1-4\frac{(\tau_{\mathrm{dir}}+1)(\tau_{\mathrm{und}}+1)-2}{\tau^2_{\mathrm{dir}}(\tau_{\mathrm{und}}+2)^2}}\right]. \tag{33}$$

As expected, the probability of an infected edge $\theta^{(\mathrm{u})}_{\vec{k}_1,\infty}$ becomes nonzero as we move away from the phase transition curve in $(\tau_{\mathrm{dir}},\tau_{\mathrm{und}})$ space, in agreement with our global spreading condition analysis [Eq. (22)]. Using our expression for $\theta^{(\mathrm{u})}_{\vec{k}_1,\infty}$, we obtain expressions for the other nonzero edge infected probabilities:

$$\theta^{(\mathrm{i})}_{\vec{k}_1,\infty} = \frac{(1-\tau_{\mathrm{und}})\theta^{(\mathrm{u})}_{\vec{k}_1,\infty}}{\tau_{\mathrm{und}}\left(1-\theta^{(\mathrm{u})}_{\vec{k}_1,\infty}\right)}, \tag{34}$$

$$\begin{aligned} \theta^{(\mathrm{i})}_{\vec{k}_3,\infty} = {} & (1-\tau_{\mathrm{dir}})\left[\theta^{(\mathrm{i})}_{\vec{k}_1,\infty}+2\theta^{(\mathrm{u})}_{\vec{k}_1,\infty}\right. \\ & \left.-2\theta^{(\mathrm{i})}_{\vec{k}_1,\infty}\theta^{(\mathrm{u})}_{\vec{k}_1,\infty}-\left(\theta^{(\mathrm{u})}_{\vec{k}_1,\infty}\right)^2+\left(\theta^{(\mathrm{i})}_{\vec{k}_1,\infty}\theta^{(\mathrm{u})}_{\vec{k}_1,\infty}\right)^2\right], \end{aligned} \tag{35}$$

and

$$\theta^{(\mathrm{u})}_{\vec{k}_4,\infty} = (1-\tau_{\mathrm{und}})\left(\theta^{(\mathrm{u})}_{\vec{k}_1,\infty}+\theta^{(\mathrm{i})}_{\vec{k}_1,\infty}-\theta^{(\mathrm{i})}_{\vec{k}_1,\infty}\theta^{(\mathrm{u})}_{\vec{k}_1,\infty}\right). \tag{36}$$

Our last step is to use the above edge infection probabilities to compute the eventual fractional extent of a global spreading event ϕ_∞ using Eq. (15) (with $\phi_0 \to 0$). In Fig. 3 we compare output of our simulations with the model's version of Eq. (15), once again showing excellent agreement.

VI. CONCLUDING REMARKS

We have provided an extensive treatment of spreading on generalized random networks, accommodating a wide range of contagion processes from biological to social in nature. Our analysis is straightforward in that physical intuition is always at hand, and in no place have we resorted to more mathematical, less transparent approaches, such as those employing generating functions.

In closing, we note that if nodes are capable of recovery and reinfection, general calculations become considerably more difficult, particularly regarding the final extent of a spreading event, and this remains an open area of investigation.

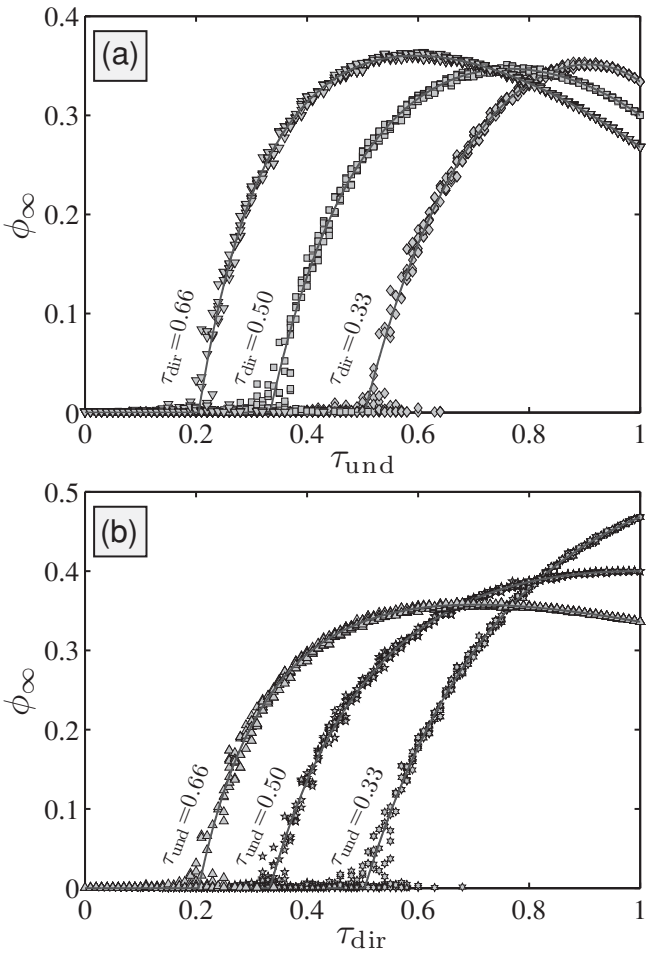

FIG. 3. Final size curves for example parameter choices for the toy model described in Sec. V with $\beta = 1$. Symbols indicate sample output from simulations with $N = 10^5$ and solid curves follow from Eqs. (15), (33), (34), (35), and (36). For each value of τ_{und} and τ_{dir} in the plots A and B, we show a maximum of 10 values of ϕ_∞ randomly chosen from 10^5 individual simulations for which the final size exceeds $\phi_\infty > 50$ (or 0.05%). The overall fit between theory and simulation is excellent. See the captions of Figs. 1 and 2 for further simulation details.

ACKNOWLEDGMENTS

JLP was supported by NIH Grant No. K25-CA134286; KDH was supported by VT-NASA EPSCoR; PSD was supported by NSF CAREER Award No. 0846668. The authors are grateful for the computational resources provided by the Vermont Advanced Computing Center which is supported by NASA (NNX 08A096G).

APPENDIX: FINAL SIZE CALCULATIONS

For the model described in Sec. V, we provide the specific forms below for Eqs. (13) and (14) as used for the calculations in Sec. V C regarding the final size of spreading events:

$$\theta^{(\mathrm{u})}_{\vec{k}_1,t+1} = \phi_0 + (1-\phi_0)\Big\{\tau_{\mathrm{und}}\Big[\big(1-\theta^{(\mathrm{i})}_{\vec{k}_1,t}\big)^2 B_{0,\vec{k}_1} + \big(1-\theta^{(\mathrm{i})}_{\vec{k}_1,t}\big)\theta^{(\mathrm{u})}_{\vec{k}_1,t} B_{1,\vec{k}_1} + \theta^{(\mathrm{i})}_{\vec{k}_1,t}\big(1-\theta^{(\mathrm{u})}_{\vec{k}_1,t}\big) B_{1,\vec{k}_1} + \theta^{(\mathrm{i})}_{\vec{k}_1,t}\theta^{(\mathrm{u})}_{\vec{k}_1,t} B_{2,\vec{k}_1}\Big] + (1-\tau_{\mathrm{und}}) B_{0,\vec{k}_4}\Big\}, \tag{A1}$$

$$\begin{aligned}\theta^{(\mathrm{i})}_{\vec{k}_1,t+1} = \phi_0 + (1-\phi_0)\Bigg\{\tau_{\mathrm{dir}}\Bigg[&\big(1-\theta^{(\mathrm{i})}_{\vec{k}_1,t}\big)\big(1-\theta^{(\mathrm{u})}_{\vec{k}_1,t}\big)^2 B_{0,\vec{k}_1} + \big(1-\theta^{(\mathrm{i})}_{\vec{k}_1,t}\big)\binom{2}{1}\theta^{(\mathrm{u})}_{\vec{k}_1,t}\big(1-\theta^{(\mathrm{u})}_{\vec{k}_1,t}\big) B_{1,\vec{k}_1} + \big(1-\theta^{(\mathrm{i})}_{\vec{k}_1,t}\big)\big(\theta^{(\mathrm{u})}_{\vec{k}_1,t}\big)^2 B_{2,\vec{k}_1} \\ &+ \theta^{(\mathrm{i})}_{\vec{k}_1,t}\binom{2}{1}\theta^{(\mathrm{u})}_{\vec{k}_1,t}\big(1-\theta^{(\mathrm{u})}_{\vec{k}_1,t}\big) B_{2,\vec{k}_1} + \theta^{(\mathrm{i})}_{\vec{k}_1,t}\big(\theta^{(\mathrm{u})}_{\vec{k}_1,t}\big)^2 B_{3,\vec{k}_1}\Bigg] + (1-\tau_{\mathrm{dir}}) B_{0,\vec{k}_2}\Bigg\},\end{aligned} \tag{A2}$$

$$\begin{aligned}\theta^{(\mathrm{i})}_{\vec{k}_3,t+1} = \phi_0 + (1-\phi_0)\Bigg\{(1-\tau_{\mathrm{dir}})\Bigg[&\big(1-\theta^{(\mathrm{i})}_{\vec{k}_1,t}\big)\big(1-\theta^{(\mathrm{u})}_{\vec{k}_1,t}\big)^2 B_{0,\vec{k}_1} + \big(1-\theta^{(\mathrm{i})}_{\vec{k}_1,t}\big)\binom{2}{1}\theta^{(\mathrm{u})}_{\vec{k}_1,t}\big(1-\theta^{(\mathrm{u})}_{\vec{k}_1,t}\big) B_{1,\vec{k}_1} + \theta^{(\mathrm{i})}_{\vec{k}_1,t}\big(1-\theta^{(\mathrm{u})}_{\vec{k}_1,t}\big)^2 B_{1,\vec{k}_1} \\ &+ \big(1-\theta^{(\mathrm{i})}_{\vec{k}_1,t}\big)\big(\theta^{(\mathrm{u})}_{\vec{k}_1,t}\big)^2 B_{2,\vec{k}_1} + \theta^{(\mathrm{i})}_{\vec{k}_1,t}\binom{2}{1}\theta^{(\mathrm{u})}_{\vec{k}_1,t}\big(1-\theta^{(\mathrm{u})}_{\vec{k}_1,t}\big) B_{2,\vec{k}_1} + \theta^{(\mathrm{i})}_{\vec{k}_1,t}\big(\theta^{(\mathrm{u})}_{\vec{k}_1,t}\big)^2 B_{3,\vec{k}_1}\Bigg] + \tau_{\mathrm{dir}} B_{0,\vec{k}_2}\Bigg\},\end{aligned} \tag{A3}$$

$$\theta^{(\mathrm{u})}_{\vec{k}_4,t+1} = \phi_0 + (1-\phi_0)\Big\{(1-\tau_{\mathrm{und}})\Big[\big(1-\theta^{(\mathrm{i})}_{\vec{k}_1,t}\big)^2 B_{0,\vec{k}_1} + \big(1-\theta^{(\mathrm{i})}_{\vec{k}_1,t}\big)\theta^{(\mathrm{u})}_{\vec{k}_1,t} B_{1,\vec{k}_1} + \theta^{(\mathrm{i})}_{\vec{k}_1,t}\big(1-\theta^{(\mathrm{u})}_{\vec{k}_1,t}\big) B_{1,\vec{k}_1} + \theta^{(\mathrm{i})}_{\vec{k}_1,t}\theta^{(\mathrm{u})}_{\vec{k}_1,t} B_{2,\vec{k}_1}\Big] + \tau_{\mathrm{und}} B_{0,\vec{k}_4}\Big\}, \tag{A4}$$

$$\theta^{(\mathrm{i})}_{\vec{k}_2} = \phi_0, \tag{A5}$$

$$\theta^{(\mathrm{i})}_{\vec{k}_4} = \phi_0. \tag{A6}$$

[1] M. E. J. Newman, SIAM Rev. **45**, 167 (2003).
[2] S. Boccaletti, V. Latora, Y. Moreno, M. Chavez, and D.-U. Hwang, Phys. Rep. **424**, 175 (2006).
[3] S. S. Shen-Orr, R. Milo, S. Mangan, and U. Alon, Nat. Genet. **31**, 64 (2002).
[4] R. Albert and A.-L. Barabási, Rev. Mod. Phys. **74**, 47 (2002).
[5] D. J. Watts, R. Muhamad, D. Medina, and P. S. Dodds, Proc. Natl. Acad. Sci. USA **102**, 11157 (2005).
[6] P. Bajardi, C. Poletto, J. J. Ramasco, M. Tizzoni, V. Colizza, and A. Vespignani, PLoS ONE **6**, e16591 (2011).
[7] S. V. Buldyrev, R. Parshani, G. Paul, H. E. Stanley, and S. Havlin, Nature (London) **464**, 1025 (2010).
[8] P. Hines, E. Cotilla-Sanchez, and S. Blumsack, Chaos **20**, 033122 (2010).
[9] D. Centola, V. M. Eguiluz, and M. W. Macy, Physica A **374**, 449 (2007).
[10] D. Centola and M. W. Macy, Am. J. Sociol. **113**, 702 (2007).
[11] D. Centola, Science **329**, 1194 (2010).
[12] M. Granovetter, Am. J. Sociol. **83**, 1420 (1978).
[13] T. Kuran, World Politics **44**, 7 (1991).
[14] T. Kuran, *Private Truths, Public Lies: The Social Consequences of Preference Falsification* (Harvard University Press, Cambridge, MA, 1997).
[15] T. C. Schelling, J. Math. Sociol. **1**, 143 (1971).
[16] T. C. Schelling, J. Conflict Resolut. **17**, 381 (1973).
[17] T. C. Schelling, *Micromotives and Macrobehavior* (Norton, New York, 1978).
[18] P. S. Dodds and D. J. Watts, Phys. Rev. Lett. **92**, 218701 (2004).
[19] D. Stauffer and A. Aharony, *Introduction to Percolation Theory*, 2nd ed. (Taylor & Francis, Washington, DC, 1992).
[20] P. S. Dodds, K. D. Harris, and J. L. Payne, Phys. Rev. E **83**, 56122 (2011).
[21] M. Boguñá and M. A. Serrano, Phys. Rev. E **72**, 016106 (2005).
[22] J. P. Gleeson and D. J. Cahalane, Phys. Rev. E **75**, 056103 (2007).
[23] J. P. Gleeson, Phys. Rev. E **77**, 046117 (2008).
[24] D. J. Watts, Proc. Natl. Acad. Sci. USA **99**, 5766 (2002).
[25] L. A. Meyers, M. Newman, and B. Pourbohloul, J. Theor. Biol. **240**, 400 (2006).
[26] Y. Ikeda, T. Hasegawa, and K. Nemoto, J. Phys.: Conf. Ser. **221**, 012005 (2010).
[27] A. Hackett, S. Melnik, and J. P. Gleeson, Phys. Rev. E **83**, 056107 (2011).
[28] J. P. Gleeson, S. Melnik, and A. Hackett, Phys. Rev. E **81**, 066114 (2010).
[29] S. Melnik, A. Hackett, M. A. Porter, P. J. Mucha, and J. P. Gleeson, Phys. Rev. E **83**, 036112 (2011).
[30] R. Milo, N. Kashtan, S. Itzkovitz, M. E. J. Newman, and U. Alon, e-print arXiv:cond-mat/0312028.
[31] P. S. Dodds and J. L. Payne, Phys. Rev. E **79**, 066115 (2009).